Supplemental Figure legends

Supplemental Figure 1. Local administration of IgG-IC does not alter mRNA expression levels of inflammatory mediators in the synovium and cause cartilage destruction in naïve mice at early stages. (**A**) Knee synovium was analyzed by qPCR for changes in mRNA levels of inflammatory mediators 1 h after i.a. injection of PBS (n = 4-6 mice), monomeric IgG (n = 3-6 mice) or IgG-IC (n = 4-7 mice). $p > 0.05$, one-way ANOVA followed by Tukey's test. (**B-C**) Representative sections of knee joint taken 1 h after i.a injection with PBS, monomeric IgG or IgG-IC, stained with TB/fast green (**B**), and scored for loss of cartilage (**C**). s: synovium. Scale bar: 100 μm. No significant difference in histology score was observed between treatments. n = 3-4 mice/group; $p > 0.05$; one-way ANOVA followed by Tukey's test.

Supplemental Figure 2. Effects of IgG-IC on joint inflammation and cartilage destruction in naïve mice at late stages. (**A**) Knee synovium was analyzed by qPCR for changes in mRNA levels of inflammatory mediators 5 h after i.a. injection of PBS (10 μl), monomeric IgG (100 μg/ml, 10 μl) or IgG-IC (100 μg/ml,10 μl). n = 3-6 mice/group; $p > 0.05$, one-way ANOVA followed by Tukey's test. (**B**) Representative knee joint sections from mice harvested 5 h after i.a injection with either PBS, monomeric IgG, or IgG-IC and stained for Ly6C/G, CD68, CD3 and c-Kit. s: synovium. Scale bar, 200 μm. (C) Quantification showed that injection of IgG-IC but not monomeric IgG caused an increase in Ly6C/G and CD3 but not other markers in the knee joint synovium compared to PBS. n = 4-5 mice/group; $*p < 0.05$, one-way ANOVA followed by Tukey's test. (**C-E**) Representative H&E and TB/fast green staining of sections of knee joints collected 5 h after i.a injection of PBS, monomeric IgG or IgG-IC and scored for synovitis and loss of cartilage. s: synovium. Scale bar, 100 μm. No significant difference in the histology score was observed between treatments. n = 3-4 mice/group; $p > 0.05$, one-way ANOVA followed by Tukey's test.

Supplemental Figure 3. Effects of immune cell depletion on mouse basal nociception. (**A**) Representative images of knee joint sections from mice injected i.a with vehicle (Veh) control liposomes (6 µl; 5 mg/ml) or clodronate-laden liposomes (6 µl; 5 mg/ml), stained for F4/80 (green). s: synovium. Scale bar, 50 µm. (**B**) Quantification showed significant reductions in synovial lining macrophages 7 days after injection of clondronate compared to vehicle. n = 4 mice/group; *p < 0.05 versus vehicle, unpaired Student t test. (**C-E**) Depletion of synovial lining macrophages with liposomal clodronate had no effects on basal mechanical sensitivity to ankle press (**C**) or plantar von Frey filament stimulation (**D**), or on basal sensitivity to plantar application of radiant heat (**E**) compared to vehicle. n = 10 mice/group; p > 0.05, unpaired Student's t test or repeated two-way ANOVA followed by Bonferroni post hoc test. (**F-K**) No significant differences were seen in basal mechanical sensitivity to ankle press (**F, I**) or plantar von Frey filament stimulation (**G**, **J**), or in basal sensitivity to plantar application of radiant heat (**H**, **K**) in mouse strains lacking either T cells (*Rag-1*$^{-/-}$) or mast cells (*c-Kit* $^{W\text{-}sh/W\text{-}sh}$), compared to WT littermates. n = 10-11 mice/group; p > 0.05, unpaired Student's t test or repeated two-way ANOVA followed by Bonferroni post hoc test.

Supplemental Figure 4. Genetic deletion of *Fcgr1* does not affect the upregulation of mRNA expression of inflammatory mediators in the AIA model. (**A-B**) qRT-PCR analysis of the mRNA expression of inflammatory mediators in the synovium of *Fcgr1*$^{+/+}$ and *Fcgr1*$^{-/-}$ mice at 7 h (**A**) and day 1 (**B**) after challenge. n = 3-9 mice/group; *p < 0.05 versus control (Ctrl), two-way ANOVA followed by Bonferroni post hoc test.

Supplemental Figure 5. Assessing the role of FcγRI in joint inflammation at day 2 following AIA. (**A**) Representative knee joint sections from *Fcgr1*$^{+/+}$ and *Fcgr1*$^{-/-}$ mice on day 2 after vehicle and mBSA challenge and stained for Ly6C/G, CD68, CD3 and c-Kit. s: synovium. Scale bar, 200 µm. (**B**) Quantification showed a significant increase in CD68, but not other immune

cell markers in the synovium following AIA. However, no significant difference in the extent of CD68 increase was observed between *Fcgr1*$^{+/+}$ and *Fcgr1*$^{-/-}$ mice. n = 3-4 mice/group; *p < 0.05 versus control, two-way ANOVA followed by Bonferroni post hoc test. (**C**) Representative images of H&E-stained knee joints on day 2 after AIA. s: synovium. Scale bar, 100 μm. (**D**) Synovitis score was increased 2 days after AIA but there was no significant difference between genotypes. n = 3-5 mice/group; *p <0.05 versus control, two-way ANOVA followed by Bonferroni post hoc test.

Supplemental Figure 6. Effects of genetic deletion of *Fcgr1* on immune cell infiltration in the synovium and cartilage destruction at day 4 after AIA. (**A**) Representative knee joint sections from *Fcgr1*$^{+/+}$ and *Fcgr1*$^{-/-}$ mice at day 4 after vehicle or mBSA challenge and stained for Ly6C/G, CD68, CD3 and c-Kit. s: synovium. Scale bar, 200 μm. (**B**) Quantification showed a significant increase in Ly6C/G, CD68, and CD3 but not c-Kit in the synovium following AIA. However, no significant difference in the increased level of the immune cell markers was observed between genotypes. n = 3-5 mice/group; *p < 0.05 versus Ctrl, two-way ANOVA followed by Bonferroni post hoc test. (**C**) Representative images of H&E-stained knee joints on day 4 after AIA. s: synovium. Scale bar, 100 μm. (**D**) Synovitis score was increased in both *Fcgr1*$^{+/+}$ and *Fcgr1*$^{-/-}$ mice at day 4 after AIA. There was no significant difference in synovitis score between genotypes. n = 4-7 mice/group; *p <0.05 versus Ctrl, two-way ANOVA followed by Bonferroni post hoc test.

Supplemental Figure 7. AIA does not cause immune cell infiltration in mouse DRG. (**A**) Representative image of mouse DRG sections from *Fcgr1*$^{+/+}$ and *Fcgr1*$^{-/-}$ mice on day 4 after AIA. DRG sections were stained for CD3 (green), Ly6C/G (green), F4/80 (green), c-Kit (green) and NeuN (red). (**B**) Quantification showed no significant difference in the number of immune

cells per unit area between groups. n = 3-4 mice/group; $p > 0.05$, two-way ANOVA followed by Bonferroni post hoc test. Scale bar, 50 μm.

Supplemental Figure 8. Genetic deletion of *Fcgr1* does not contribute to cartilage destruction in the AIA model. (**A-B**) Representative images of TB/fast green-stained knee joints from *Fcgr1*$^{+/+}$ and *Fcgr1*$^{-/-}$ mice on days 2 (**A**) and 4 (**B**) after AIA. s: synovium. Scale bar, 100 μm. (**C-D**) No obvious difference in the histology score for cartilage destruction was observed at days 2 (**C**) and 4 (**D**) after AIA between any groups. n = 4-5 mice/group; $p > 0.05$ versus Ctrl, two-way ANOVA followed by Bonferroni post hoc test.

Supplemental Figure 9. Genetic deletion of *Fcgr1* in sensory neurons attenuates AIA-associated pain in female mice. (**A-E**) Time course of ankle mechanical threshold (**A**), paw withdrawal frequency (PWF) to 0.07 g (**B**) and 0.4 g force (**C**), paw withdrawal latency to radiant heat (**D**), and ankle joint diameter (**E**) following AIA in *PirtCre; Fcgr1*$^{fl/fl}$ mice (n = 7 mice) and *Fcgr1*$^{fl/fl}$ control littermates (n = 10 mice); *$p < 0.05$ versus *Fcgr1*$^{fl/fl}$ controls, #$p < 0.05$ versus day 0, two-way repeated measures ANOVA followed by Bonferroni post hoc test.

Supplemental Figure 10. Acute pharmacological blockade of FcγRI reverses AIA-associated pain in female mice. (**A-E**) Effects of repeated daily i.a injection of anti-CD64 (2.25 μg, 5 μl; n = 9 mice) or IgG2b isotype control (2.25 μg, 5 μl; n = 8 mice) on mechanical threshold in the ankle (**A**), paw withdrawal frequency (PWF) in response to 0.07 g (**B**) and 0.4 g force (**C**), paw withdraw latency to radiate heat (**D**), and ankle joint diameter (**E**) in mice with AIA. *$p< 0.05$ versus control IgG2b isotype; #$p < 0.05$, versus day 0; two-way ANOVA for repeated measures followed by Bonferroni post hoc test.

Supplemental information of methods

Antigen-induced arthritis (AIA)

Methylated bovine serum albumin (mBSA, Sigma, St. Louis, MO), was used as an antigen to elicit arthritis in the mouse as a model of human RA, as described previously (32, 33). Briefly, mice were sensitized with 500 µg of mBSA in 200 µl of an emulsion containing 100 µl saline and 100 µl complete Freund's adjuvant (CFA, 1 mg/ml; Sigma, St Louis, MO) and delivered by subcutaneous (s.c.) injection to the caudal back skin using a sterile syringe and 25 G needle. Mice were boosted with the same preparations on day 7. Immunized mice were challenged on day 21 by intraarticular (i.a.) injection of mBSA (30 µg; 10 µl in saline) or saline alone (vehicle) to the right ankle (for behavioral testing, in vivo imaging and electrophysiological recordings, and in vitro), or knee (for joint histology and real-time PCR on synovium tissue) of the hindlimb. Ankle diameter was measured with digital calipers as an indicator of joint inflammation.

Complete Freund Adjuvant (CFA)-induced arthritis

Joint inflammation was induced by injection of CFA (Sigma, St. Louis, MO) into the cavity of the right hind ankle (5 µl) of mice under isoflurane anesthesia as previously described (36, 37). Joint inflammation and pain related behaviors were assessed over a 4 week period.

Formalin-induced hindpaw inflammation

Formalin (20 µl, 5% in saline) was subcutaneously injected into the plantar surface of the right hindpaw of awake mice. Behavioral responses were video recorded with a camcorder for 1h. The video recording was played back offline in slow-motion to assess the time spent lifting, biting and licking the right hindpaw. Behavioral responses were compared by pooling data in the first (0-10 min) and second (11-60 min) phases.

Behavioral testing

All behavioral measurements were done in awake, unrestrained and age-matched littermates (2-3 months) by experimenters blinded to the genotype and treatment. Primary mechanical hyperalgesia in both ankle joints was measured by applying ascending forces to the ankle with electronic blunt forceps (IITC Life Science Inc., Woodland Hills, CA). The cutoff force was set at 300 g to avoid joint damage. The mechanical threshold was defined as the force at which the mouse withdrew its hindlimb forcefully or vocalized (33). The mechanical threshold in the joint was averaged over three measurements obtained at intervals of at least 5 min. Secondary mechanical hyperalgesia in the glabrous skin of both hindpaws was evaluated using von Frey monofilaments of different forces ranging from 0.07 to 1.4 g. Paw withdrawal responses to ten applications of each filament were counted. Secondary thermal hyperalgesia in the glabrous hind paw skin was assessed by measuring withdrawal latency to noxious heat stimuli delivered using a radiant heat source (Plantar Test Apparatus, IITC Life Science Inc., Woodland Hills, CA). The cutoff latency was set at 15 s. Heat response latencies were averaged over three measurements obtained at intervals of at least 3 min.

DRG neuronal culture and calcium imaging

L4-L5 lumbar DRG from WT and global *Fcgr1*$^{-/-}$ knockout mice, and saline- or mBSA-treated mice , were harvested and placed in oxygenated complete saline solution (CSS) for cleaning and then mincing (33). CSS consisted of (in mM): 137 NaCl, 5.3 KCl, 1 $MgCl_2$, 3 $CaCl_2$, 25 Sorbitol, and 10 HEPES, adjusted to pH 7.2 with NaOH. For 20 min the DRGs were digested with 0.35 U/ml Liberase TM (Roche Diagnostics Corp., Indianapolis, IN) and then for 15 min with Liberase TL (0.25 U/ml; Roche Diagnostics Corp., IN) and papain (30 U/ml, Worthington Biochemical, Lakewood, NJ) in CSS containing 0.5 mM EDTA at 37°C. The tissue was triturated with a fire-polished Pasteur pipette. The DRG neurons were suspended in complete DRG medium containing 1 mg/ml trypsin inhibitor and 1 mg/ml bovine serum albumin (Sigma, St. Louis, MO) and then plated onto poly-D-lysine/laminin coated glass coverslips. The complete

DRG medium contained equivalent amounts of DMEM and F12 (Life Technologies Corp., Grand Island, NY) with 10% FCS (Sigma, St. Louis, MO) and 1% penicillin and streptomycin (Invitrogen). The cells were then maintained in 5% CO_2 at 37^{o}C in a humidified incubator. At 16-24 h after plating, neurons were loaded with Fura-2 (10 μM) in the dark for 30 min and subsequently washed twice in a HEPES buffer containing (in mM): 145 NaCl, 3 KCl, 2 $MgCl_2$, 2 $CaCl_2$, 10 glucose and 10 HEPES (adjusted to pH 7.4 with NaOH). Cells were alternately excited at 340 nm and 380 nm, with exposure times adjusted to correct for differential efficiency of illumination, and image pairs were acquired at 2 s intervals. F340/380 ratio was calculated as described previously (28). IgG-IC, antigen (BSA), or antibody (anti-BSA), each at the dose of 1 μg/ml, was applied. Capsaicin (1 μM; Sigma, St. Louis, MO) and 50 mM KCl were applied at the end of each experiment.

Depletion of synovial macrophages

Synovial lining macrophages were depleted using a standard macrophages depletion kit (Encapsula NanoSciences LLC; Brentwood, TN) as described previously (31, 32). Briefly, 6 μl of a clodronate-laden liposome suspension (5 mg/ml) was injected into the knee (for IHC staining) or ankle (for behavioral testing) joint cavity of mice 7 days before behavioral measurement (31, 32). Liposomes lacking clodronate served as the vehicle control. The efficiency of macrophage depletion was evaluated by immunostaining the knee synovial lining with the macrophage marker anti-F4/80.

Quantitative real-time PCR (qRT-PCR)

RNA was extracted from L3-L5 DRGs, or from the synovium of mice using a standard Trizol extraction method and RNA quantity was measured using a NanoDrop 1000 (Thermo Fisher Scientific, Waltham, MA). RNA was then reverse-transcribed to complimentary DNA using the iScript cDNA synthesis kit (Bio-Rad, Hercules, CA) according to the manufacturer's protocol.

For relative quantification of mRNA, RT-PCR was performed on a QuantStudio 3 real-time PCR system (Applied Biosciences Corp., Beverly Hills, CA) using PowerUp SYBR Green Master Mix (Applied Biosciences Corp., Beverly Hills, CA). The primers used are summarized in Table S1. Each sample was performed in duplicate. The expression levels of the target genes were quantified relative to the level of β-actin gene expression using the $2^{-\Delta\Delta CT}$ method.

Immunohistochemistry (IHC)

Anesthetized mice were transcardially perfused with PBS, followed by 4% paraformaldehyde (PFA). L4-L5 DRGs, knee joint and spleen were dissected, cryopreserved in 30% sucrose and cryosectioned at 14 µm (DRG and spleen) or 16 µm (knee joint). After blocking, sections were incubated with primary antibodies (Table S2) overnight at 4°C. Sections were then washed and incubated with complementary secondary antibodies (Table S2) at RT for 2 hrs. Images were captured using a confocal microscope (Nikon A1+ or Zeiss LSM 710).

Confocal imaging analysis

All images were analyzed using NIS elements or ImageJ software in a blinded manner. For joint tissue, 2-3 sections per animal were imaged. For each marker, the synovium was chosen as region of interest (ROI) and the fluorescence intensity per unit area was used for signal quantification. For ISH on DRG, 2-4 sections of the L4-L5 DRG per animal were analyzed for the quantification of DRG neuron subpopulations. The number of cells for each marker was assessed as a percentage of all FB-labeled FcγRI positive cells unless specified. However, for DRG tissue from *PirtCre; Fcgr1*$^{fl/fl}$ mice, signal fluorescence intensity per unit area was measured instead. For ISH on spleen tissue, 2-3 sections per animal were analyzed and the signal fluorescence intensity per unit area was measured. For analysis of immune cell infiltration in DRG, 3-4 sections of L4-L5 DRG per animal were imaged and the number of cells immunopositive for each marker (CD3, Ly6C/G, F4/80 and c-Kit) per unit area was counted. For

each marker within a group, all parameters for image acquisition and analysis were kept constant across the images.

In vivo DRG electrophysiological recordings

The properties of DRG neurons innervating the hind limb ankles of mice were recorded in vivo on day 1 after the induction of AIA using extracellular recording as described (33). Briefly, under isoflurane anesthesia delivered via intratracheal ventilation (SomnoSuite, Kent Scientific Corp., Torrington, CT), the lumbar spinal column was exposed and a laminectomy was performed at the L2-L6 levels. The L4 DRG was exposed and superfused with oxygenated artificial cerebrospinal fluid (ACSF) within a pool formed by a ring to which the skin was sewn. ACSF contained (in mM): 130 NaCl, 3.5 KCl, 24 $NaHCO_3$, 1.25 NaH_2PO_4, 1.2 $MgCl_2$, 1.2 $CaCl_2$, and 10 dextrose, was bubbled with 95% O_2 and 5% CO_2 and had a pH of 7.4 and an osmolality of 290~310 mOsm. After removal of the epineurium, the neurons on the surface of the DRG were viewed by reflection microscopy on a Nikon FN1 upright microscope equipped with a mercury light source (Nikon, Mellvile, NY) and an infrared camera (DAGE-MTI, Michigan City, IN). Epifluorescence imaging was also used to identify DiI-labeled joint-innervating neurons.

Extracellular recordings were made on individual DRG cell bodies using a polished suction micropipette electrode with a tip of 20-30 μm. Pipettes were pulled from borosilicate glass capillaries (Sutter Instruments; Novato, CA) using a P97 micropipette puller (Sutter Instruments; Novato, CA). The occurrence of action potentials (APs) was recorded extracellularly using a Multiclamp 700B amplifier and pCLAMP10 software (Molecular Device, Sunnyvale, CA). The peripheral receptive field (RF) of an individual joint-innervating DRG neuron was identified by probing the skin over and around the exposed ankle with a hand-held blunt glass probe. Only DRG neurons that had a mechanical RF in the ankle were included. The mechanical sensitivity of joint sensory afferents was assessed by poking their RF with a set of calibrated von Frey monofilaments with a fixed tip diameter (100 μm). Each monofilament was applied for 2 s with

an inter-stimulus interval of 3 min. Mechanical responses were quantified as the mean number of evoked APs during 2 s mechanical stimulation. The neuron was classified as spontaneously active only if spontaneous ongoing discharges occurred during a 3 min period without any external stimulation. Afterdischarge was defined as APs observed in 2 min immediately after removal of a mechanical stimulus from the RF. To avoid the confounds of abnormal activity, force-AP relations were analyzed only in neurons that exhibited neither SA nor mechanically-evoked afterdischarges. Conduction velocity (CV) was obtained by electrically stimulating the RF with two wire electrodes and calculated by dividing the conduction distance between the stimulation electrode and the soma of the recorded neurons by the latency to a spike peak. For this study, C fiber and Aδ nociceptors were preferentially studied.

In vivo DRG calcium imaging

WT and global *Fcgr1*$^{-/-}$ mice on a *PirtCre-GCamp6* background were used for this study. One week after DiI injection into the ankle joint, a mouse was deeply anesthetized using chloral hydrate (i.p.; 560 mg/kg; Sigma). The L4 DRG was exposed as described above but without removal of the epineurium covering the DRG. The vertebrae were stabilized at two sites using custom designed clamps. Images were acquired using a confocal microscope (Leica LSI microscope system) equipped with a 0.5 N.A. macro dry objective and fast EM-CCD camera, or a confocal fluorescence microscope (Nikon A1+; Nikon, Mellvile, NY) using a 10x water immersion lens as reported previously (30). A 488 nm Argon ion laser line was used for excitation and GCamp6 signal was recorded at 500-550 nm. Z-stacks were used to capture the entire area of the DRG in 8-11 steps over a distance of 200-300 μm at 512 x 512 pixel resolution in the X-Y plane. For each stimulus, 20-30 z-stacks were taken and each stack took 20-30 s to achieve. To avoid the potential priming effects of different chemicals, only a single agent (IgG-IC, 100 μg/ ml, 10 ul; monomeric IgG, 100 μg/ ml, 10 ul; or PBS, 10 ul), was injected

into the right ankle joint cavity of any given animal. Mechanical force was applied to the ankle using forceps at the end of each experiment. The interval between stimuli was 3-5 min.

Calcium imaging was analyzed using ImageJ. The observer was blinded to the treatment and mouse genotype. The ImageJ Linear Stack Alignment plug-in was used to correct for movement artifacts. All DiI-labeled DRG neurons that showed increased fluorescence upon stimulus application were defined as region of interest (ROI) for further analysis. Neurons showing spontaneous activity without any stimuli were excluded. Neurons were considered responsive to any stimulus if $\Delta F / F_o > 15\%$, where F_o is the average basal intensity before stimulus application (30).

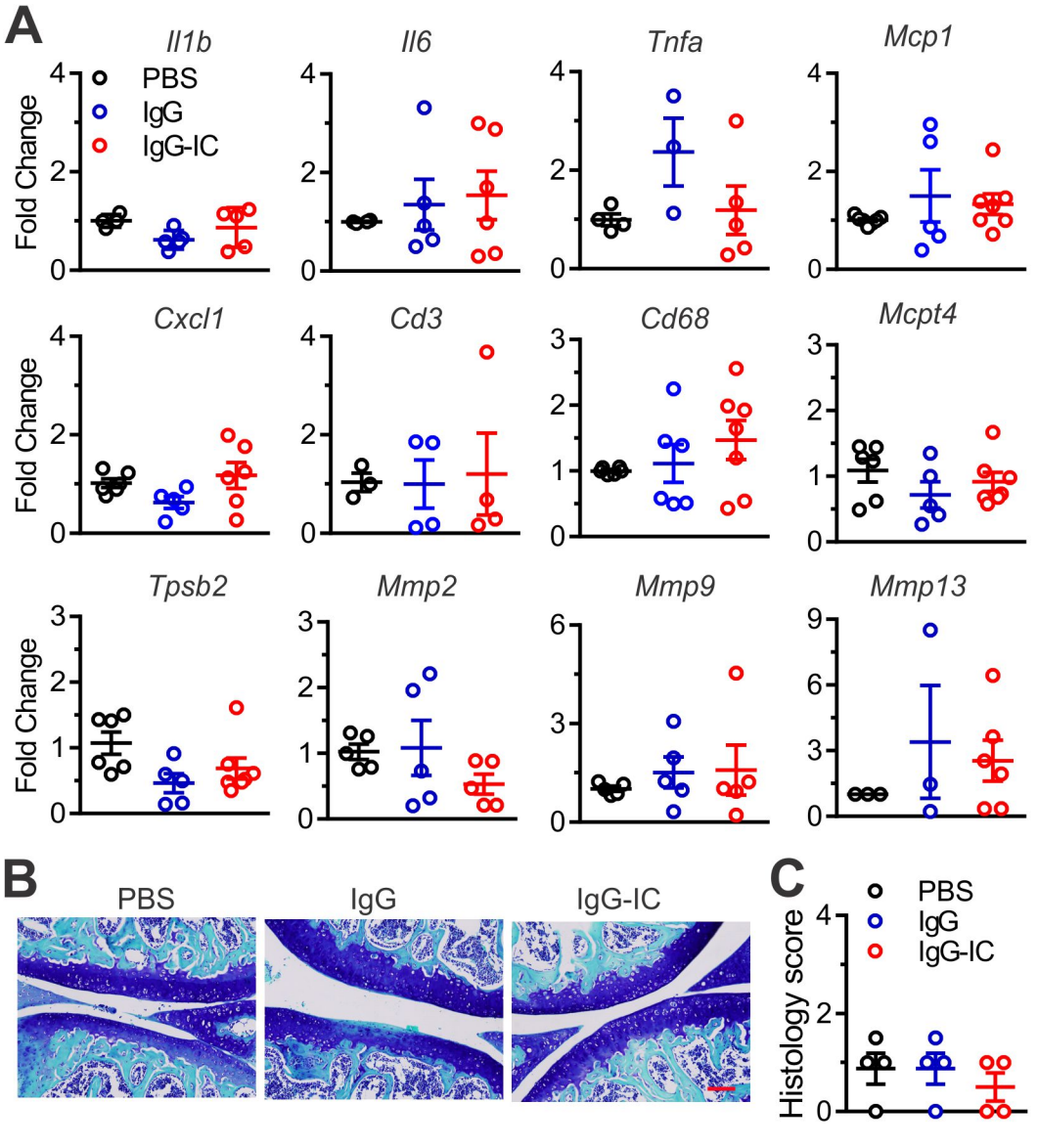
A
Il1b
Il6
Tnfa
Mcp1
Cxcl1
Cd3
Cd68
Mcpt4
Tpsb2
Mmp2
Mmp9
Mmp13
PBS
IgG
IgG-IC
Fold Change
B
PBS
IgG
IgG-IC
C
Histology score

S. Fig. 2

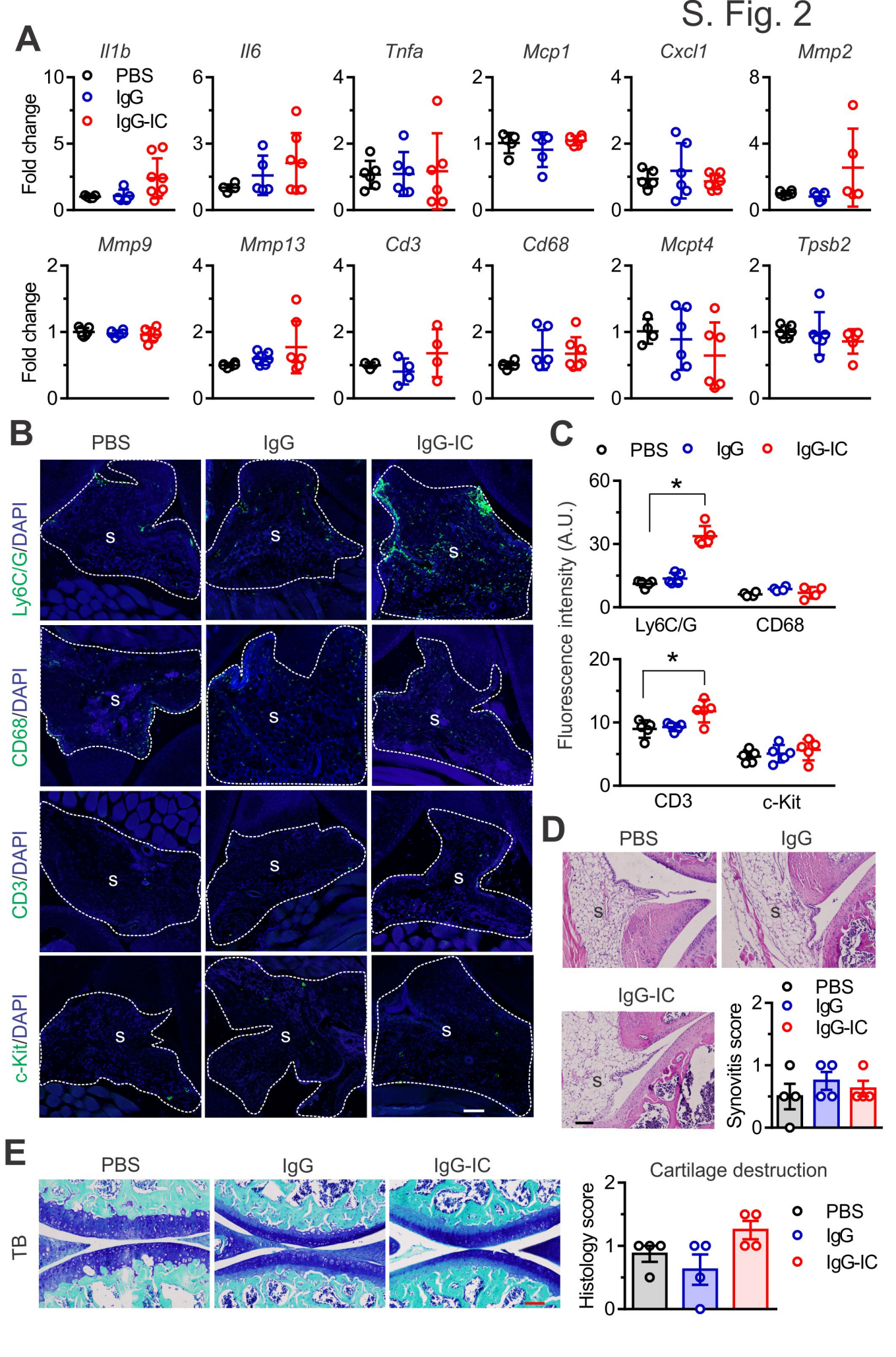
A
Il1b
Il6
Tnfa
Mcp1
Cxcl1
Mmp2
Mmp9
Mmp13
Cd3
Cd68
Mcpt4
Tpsb2
PBS
IgG
IgG-IC
Fold change
B
PBS
IgG
IgG-IC
Ly6C/G/DAPI
CD68/DAPI
CD3/DAPI
c-Kit/DAPI
S
C
PBS
IgG
IgG-IC
Fluorescence intensity (A.U.)
Ly6C/G
CD68
CD3
c-Kit
D
PBS
IgG
IgG-IC
Synovitis score
E
PBS
IgG
IgG-IC
TB
Cartilage destruction
Histology score

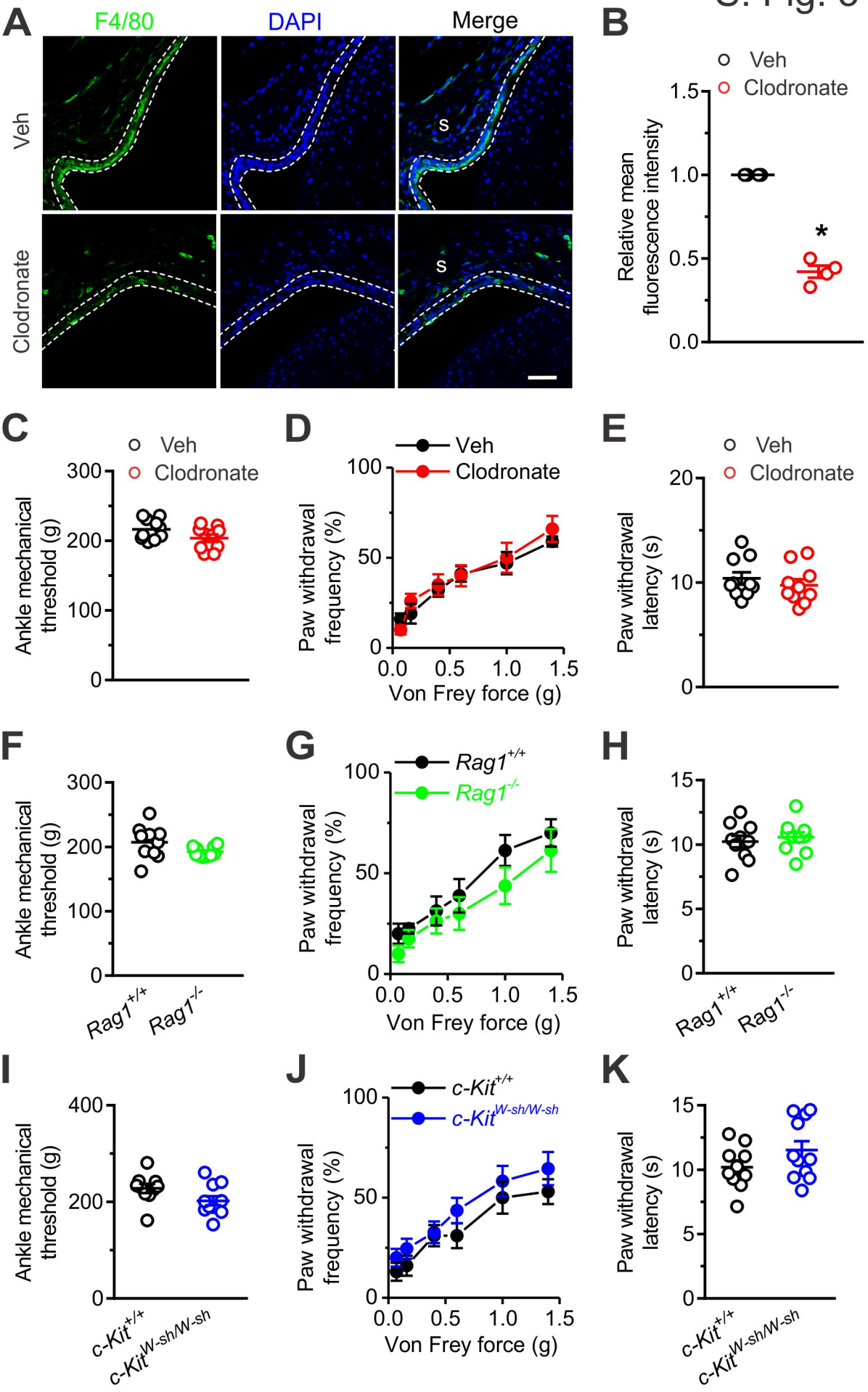
A
F4/80
DAPI
Merge
Veh
Clodronate
s
B
Veh
Clodronate
Relative mean fluorescence intensity
1.5
1.0
0.5
0.0
*
C
Veh
Clodronate
Ankle mechanical threshold (g)
300
200
100
0
D
Veh
Clodronate
Paw withdrawal frequency (%)
100
50
0
0.0
0.5
1.0
1.5
Von Frey force (g)
E
Veh
Clodronate
Paw withdrawal latency (s)
20
10
0
F
Ankle mechanical threshold (g)
300
200
100
0
Rag1+/+
Rag1-/-
G
Rag1+/+
Rag1-/-
Paw withdrawal frequency (%)
100
50
0
0.0
0.5
1.0
1.5
Von Frey force (g)
H
Paw withdrawal latency (s)
15
10
5
0
Rag1+/+
Rag1-/-
I
Ankle mechanical threshold (g)
400
200
0
c-Kit+/+
c-KitW-sh/W-sh
J
c-Kit+/+
c-KitW-sh/W-sh
Paw withdrawal frequency (%)
100
50
0
0.0
0.5
1.0
1.5
Von Frey force (g)
K
Paw withdrawal latency (s)
15
10
5
0
c-Kit+/+
c-KitW-sh/W-sh

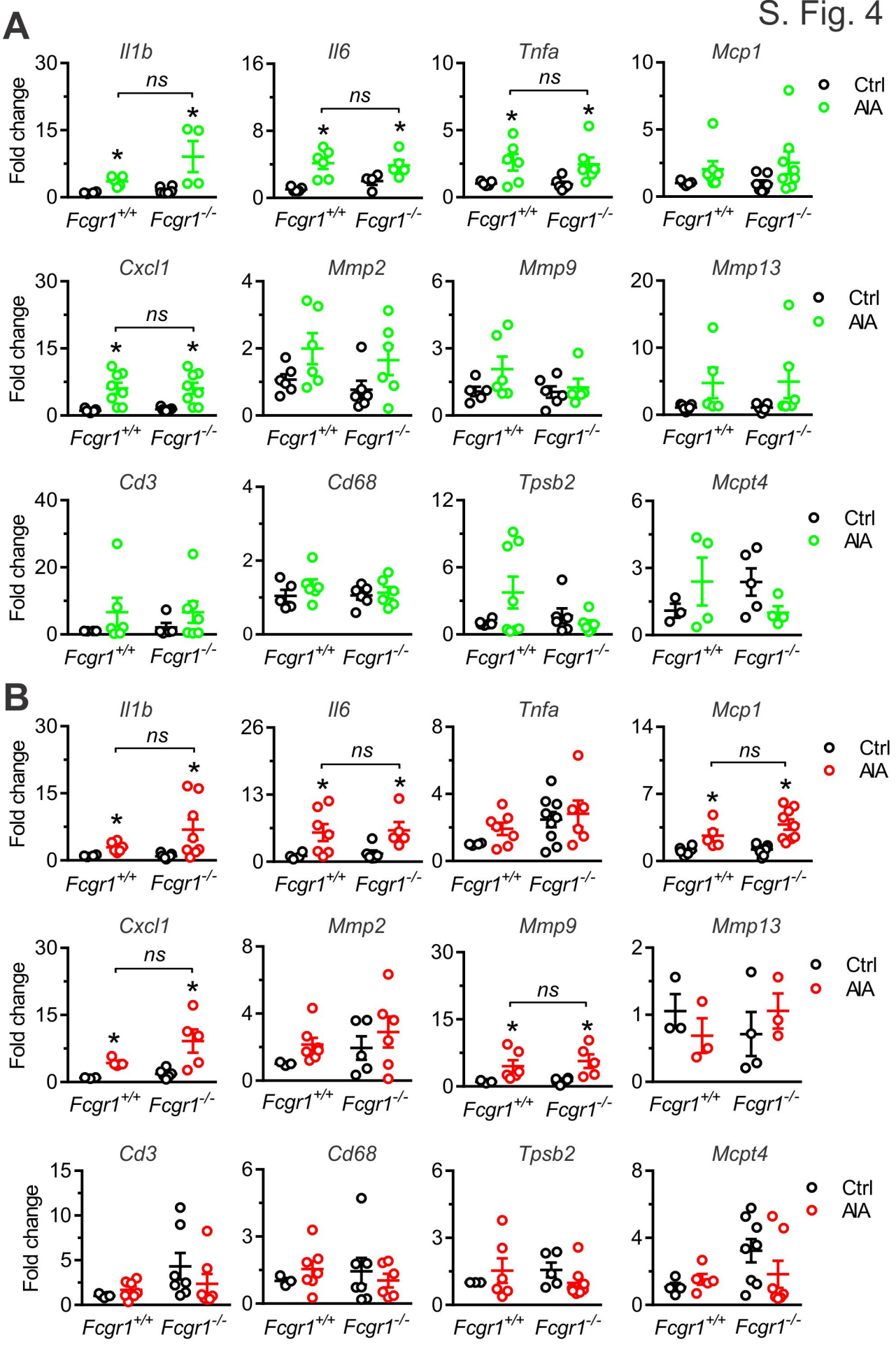
A
Il1b
Il6
Tnfa
Mcp1
Cxcl1
Mmp2
Mmp9
Mmp13
Cd3
Cd68
Tpsb2
Mcpt4
Fold change
ns
*
Ctrl
AIA
Fcgr1+/+
Fcgr1-/-
B
Il1b
Il6
Tnfa
Mcp1
Cxcl1
Mmp2
Mmp9
Mmp13
Cd3
Cd68
Tpsb2
Mcpt4
Fold change
ns
*
Ctrl
AIA
Fcgr1+/+
Fcgr1-/-

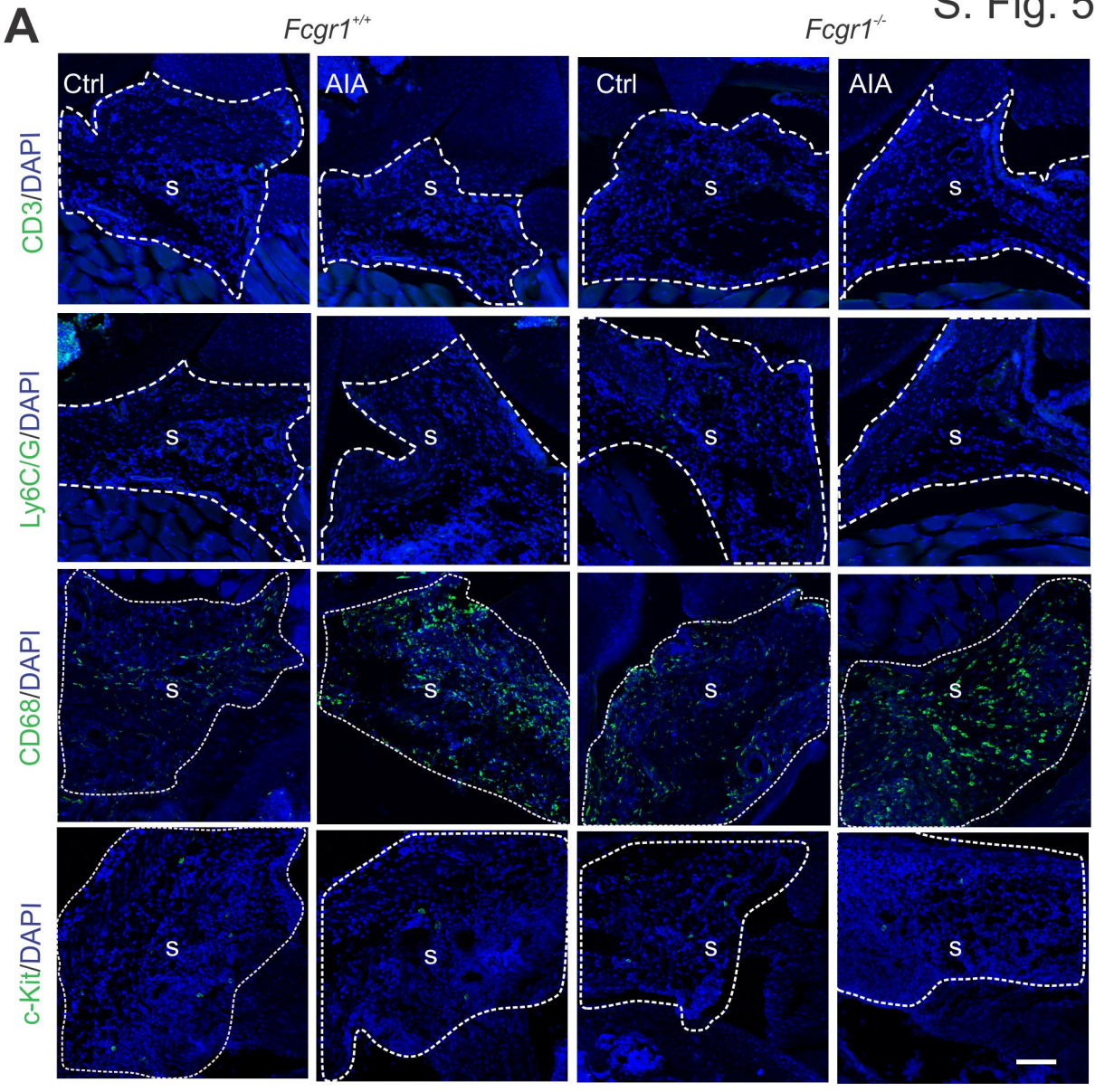
A
Fcgr1+/+
Fcgr1-/-
Ctrl
AIA
Ctrl
AIA
CD3/DAPI
Ly6C/G/DAPI
CD68/DAPI
c-Kit/DAPI
s

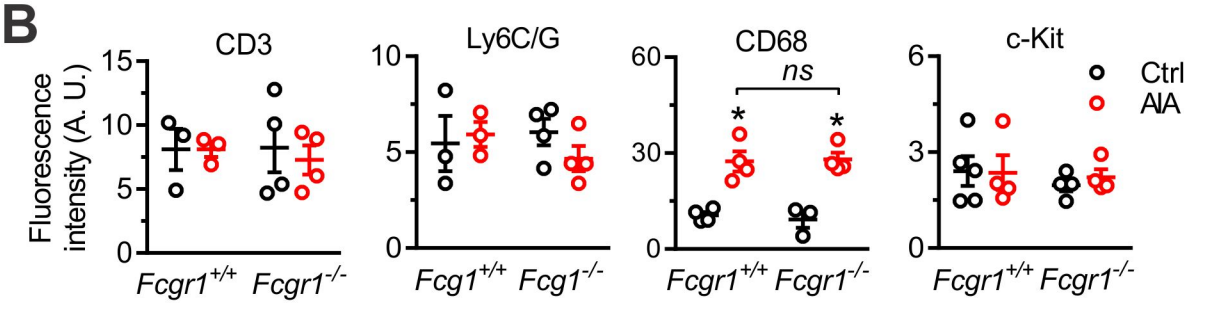
B
CD3
Ly6C/G
CD68
c-Kit
ns
Ctrl
AIA
Fluorescence intensity (A. U.)
Fcgr1+/+ Fcgr1-/-
Fcg1+/+ Fcg1-/-

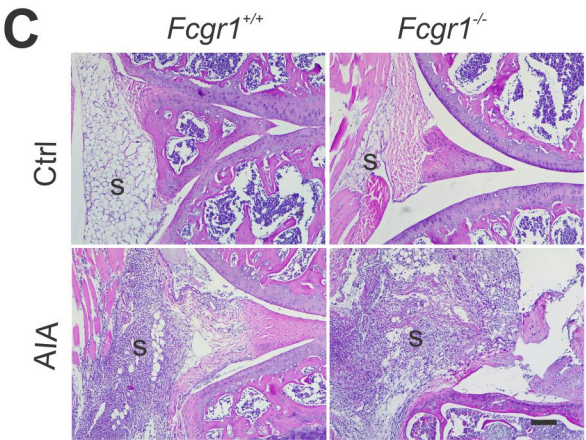
C
Fcgr1+/+
Fcgr1-/-
Ctrl
AIA
s

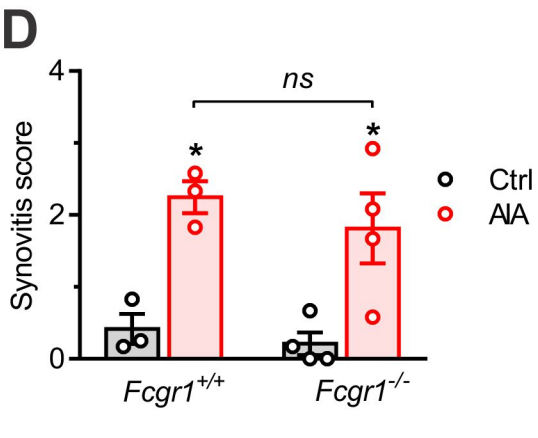
D
ns
Synovitis score
Ctrl
AIA
Fcgr1+/+
Fcgr1-/-

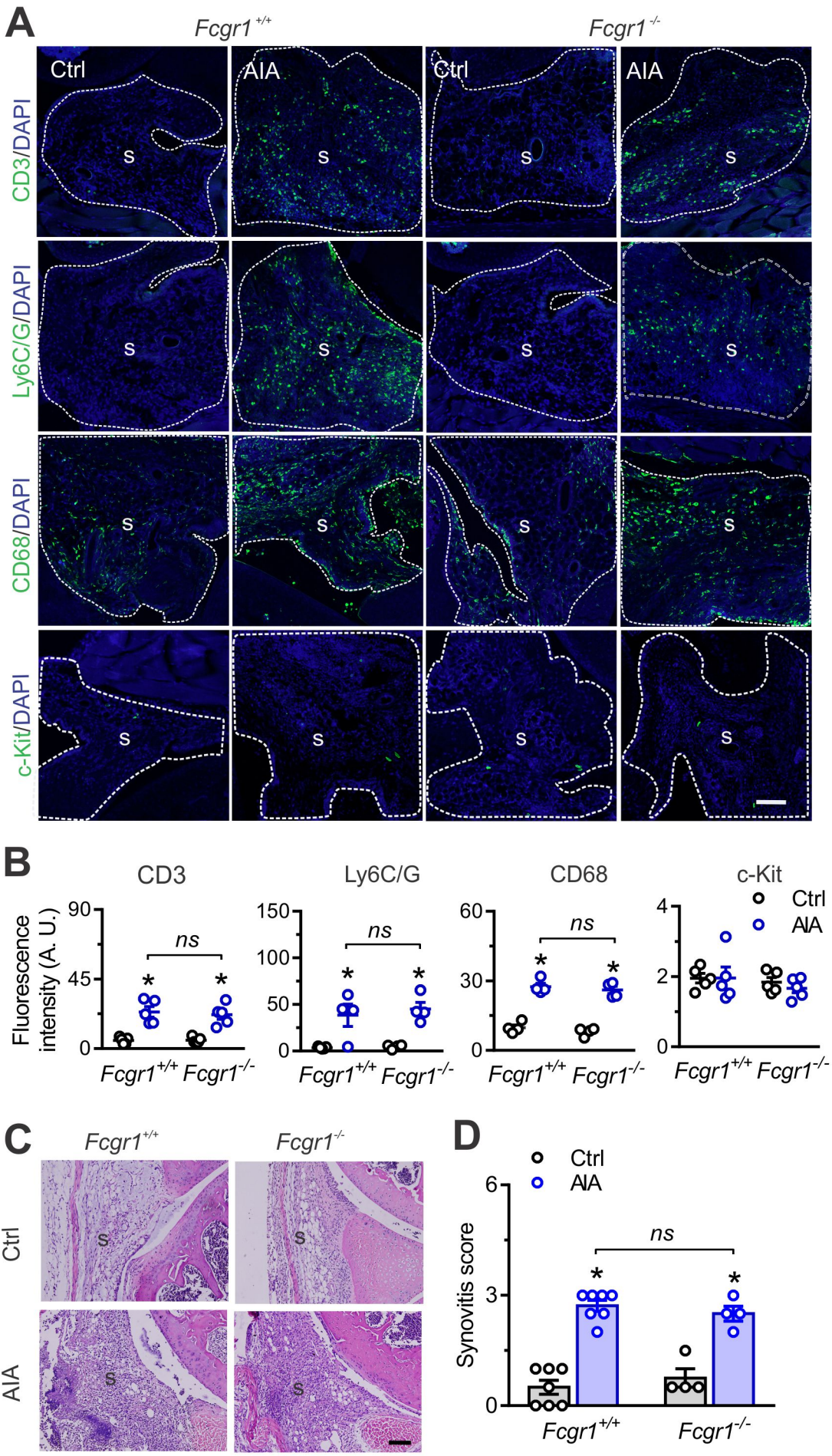
A
Fcgr1+/+
Fcgr1-/-
Ctrl
AIA
Ctrl
AIA
CD3/DAPI
Ly6C/G/DAPI
CD68/DAPI
c-Kit/DAPI
S
B
CD3
Ly6C/G
CD68
c-Kit
Ctrl
AIA
Fluorescence intensity (A. U.)
90
45
0
150
100
50
0
60
30
0
4
2
0
ns
*
Fcgr1+/+
Fcgr1-/-
C
Fcgr1+/+
Fcgr1-/-
Ctrl
AIA
S
D
Ctrl
AIA
Synovitis score
6
3
0
ns
*
Fcgr1+/+
Fcgr1-/-

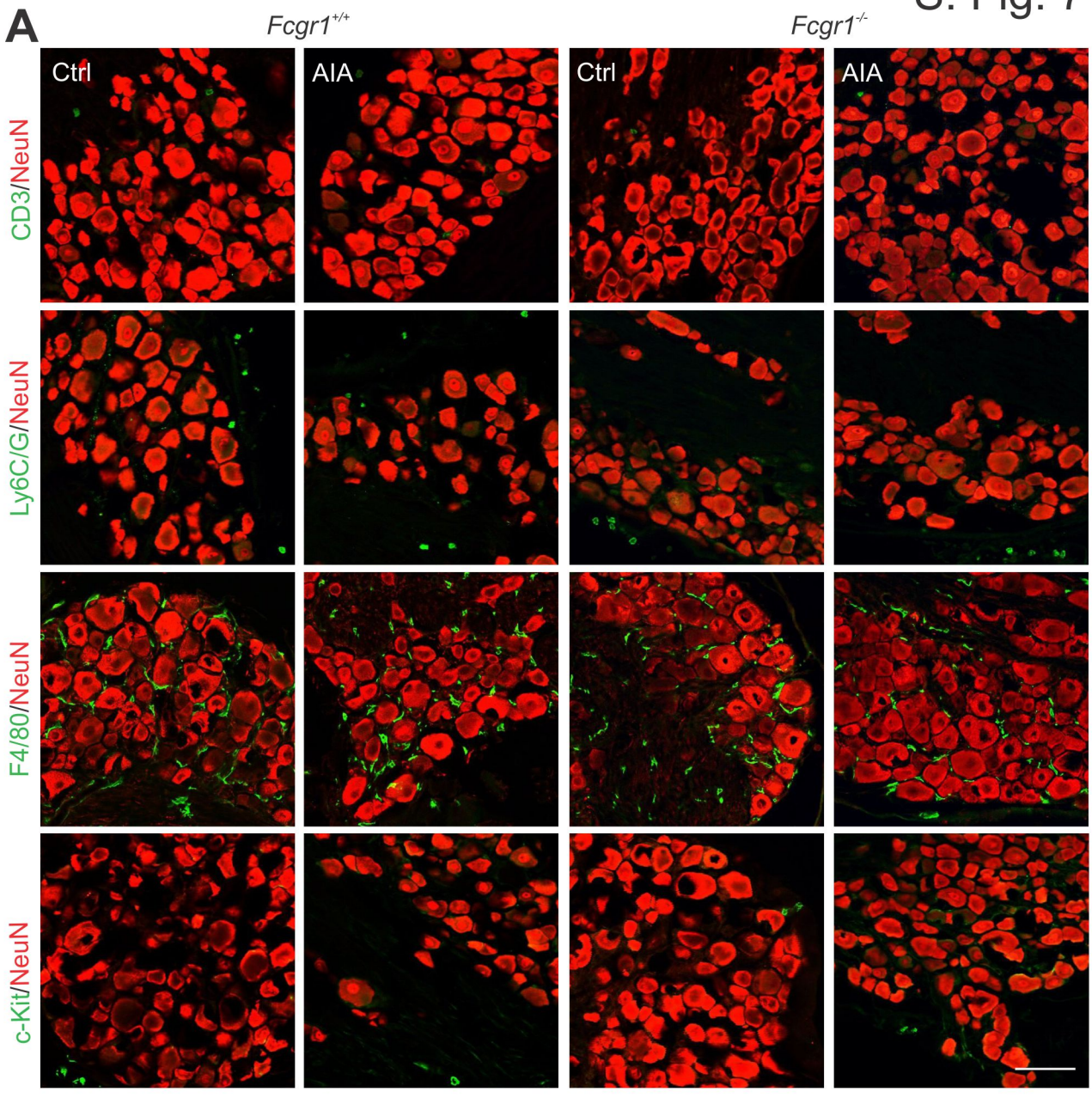
A
Fcgr1+/+
Fcgr1-/-
Ctrl
AIA
Ctrl
AIA
CD3/NeuN
Ly6C/G/NeuN
F4/80/NeuN
c-Kit/NeuN

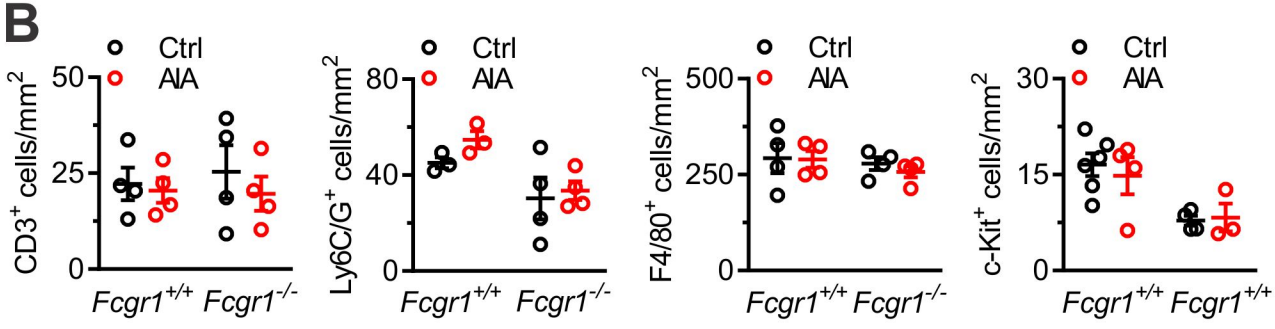
B
Ctrl
AIA
CD3+ cells/mm2
50
25
0
Fcgr1+/+ Fcgr1-/-
Ly6C/G+ cells/mm2
80
40
0
F4/80+ cells/mm2
500
250
c-Kit+ cells/mm2
30
15

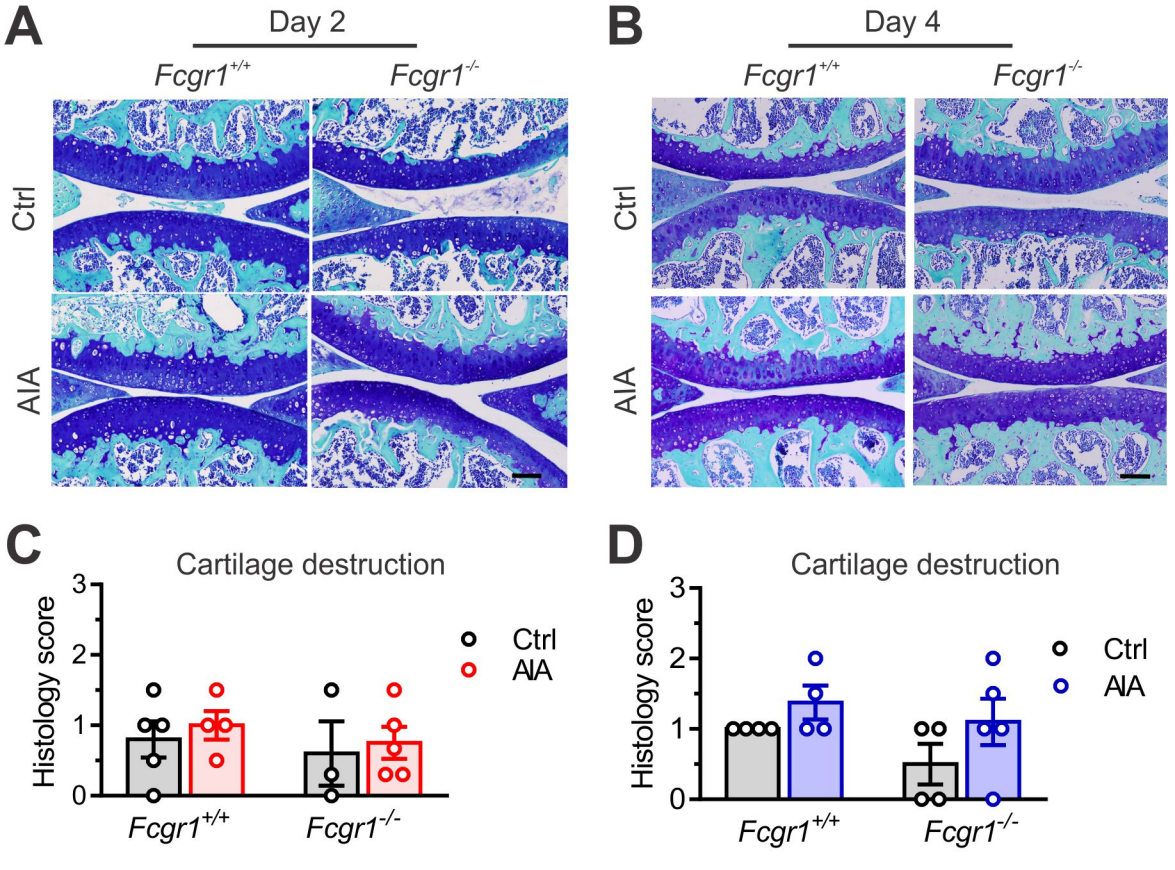
A
Day 2
Fcgr1+/+
Fcgr1-/-
Ctrl
AIA
B
Day 4
Fcgr1+/+
Fcgr1-/-
Ctrl
AIA
C
Cartilage destruction
Histology score
0
1
2
3
Ctrl
AIA
Fcgr1+/+
Fcgr1-/-
D
Cartilage destruction
Histology score
0
1
2
3
Ctrl
AIA
Fcgr1+/+
Fcgr1-/-

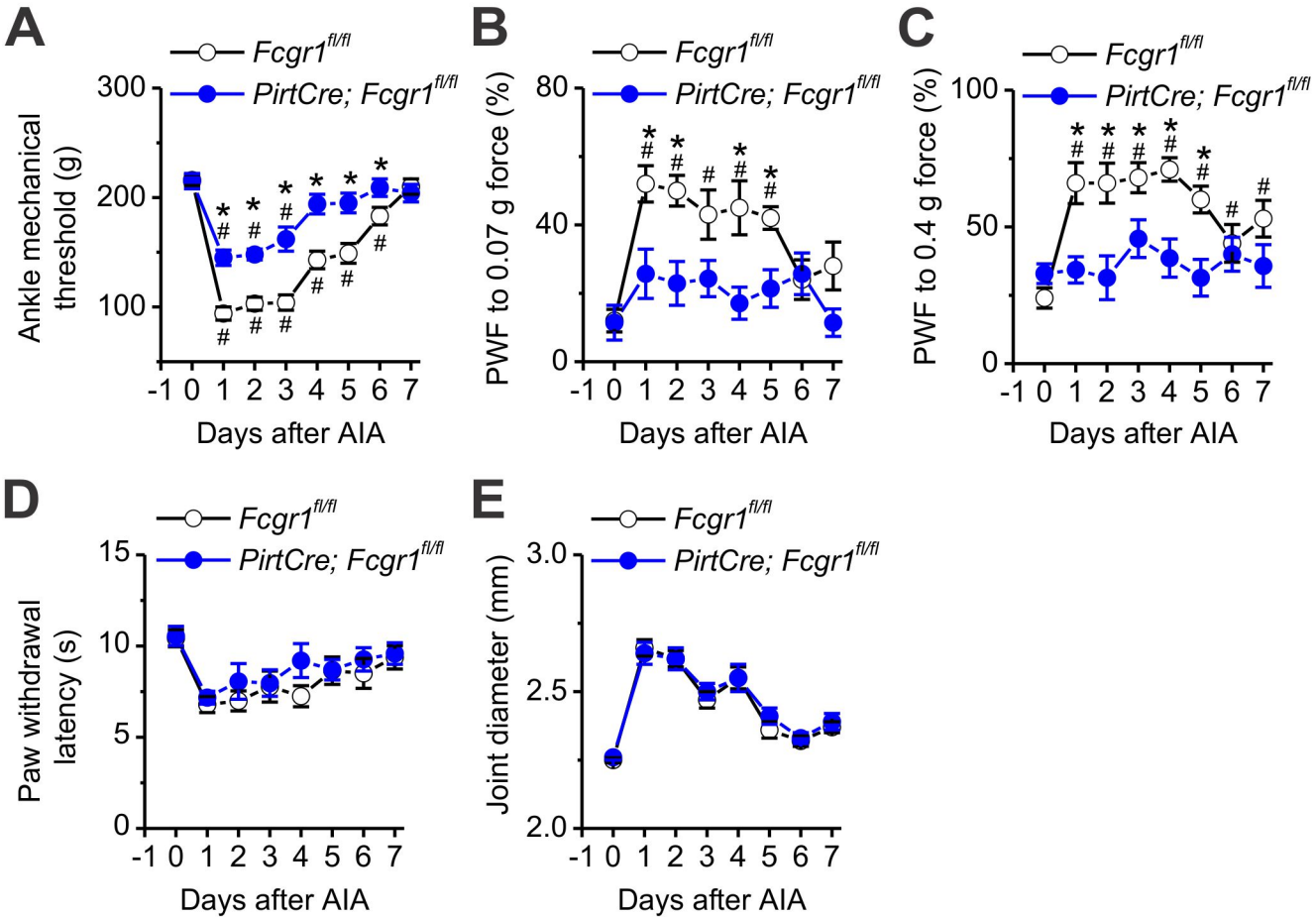
A
Fcgr1fl/fl
PirtCre; Fcgr1fl/fl
Ankle mechanical threshold (g)
300
200
100
-1 0 1 2 3 4 5 6 7
Days after AIA
B
Fcgr1fl/fl
PirtCre; Fcgr1fl/fl
PWF to 0.07 g force (%)
80
40
0
-1 0 1 2 3 4 5 6 7
Days after AIA
C
Fcgr1fl/fl
PirtCre; Fcgr1fl/fl
PWF to 0.4 g force (%)
100
50
0
-1 0 1 2 3 4 5 6 7
Days after AIA
D
Fcgr1fl/fl
PirtCre; Fcgr1fl/fl
Paw withdrawal latency (s)
15
10
5
0
-1 0 1 2 3 4 5 6 7
Days after AIA
E
Fcgr1fl/fl
PirtCre; Fcgr1fl/fl
Joint diameter (mm)
3.0
2.5
2.0
-1 0 1 2 3 4 5 6 7
Days after AIA

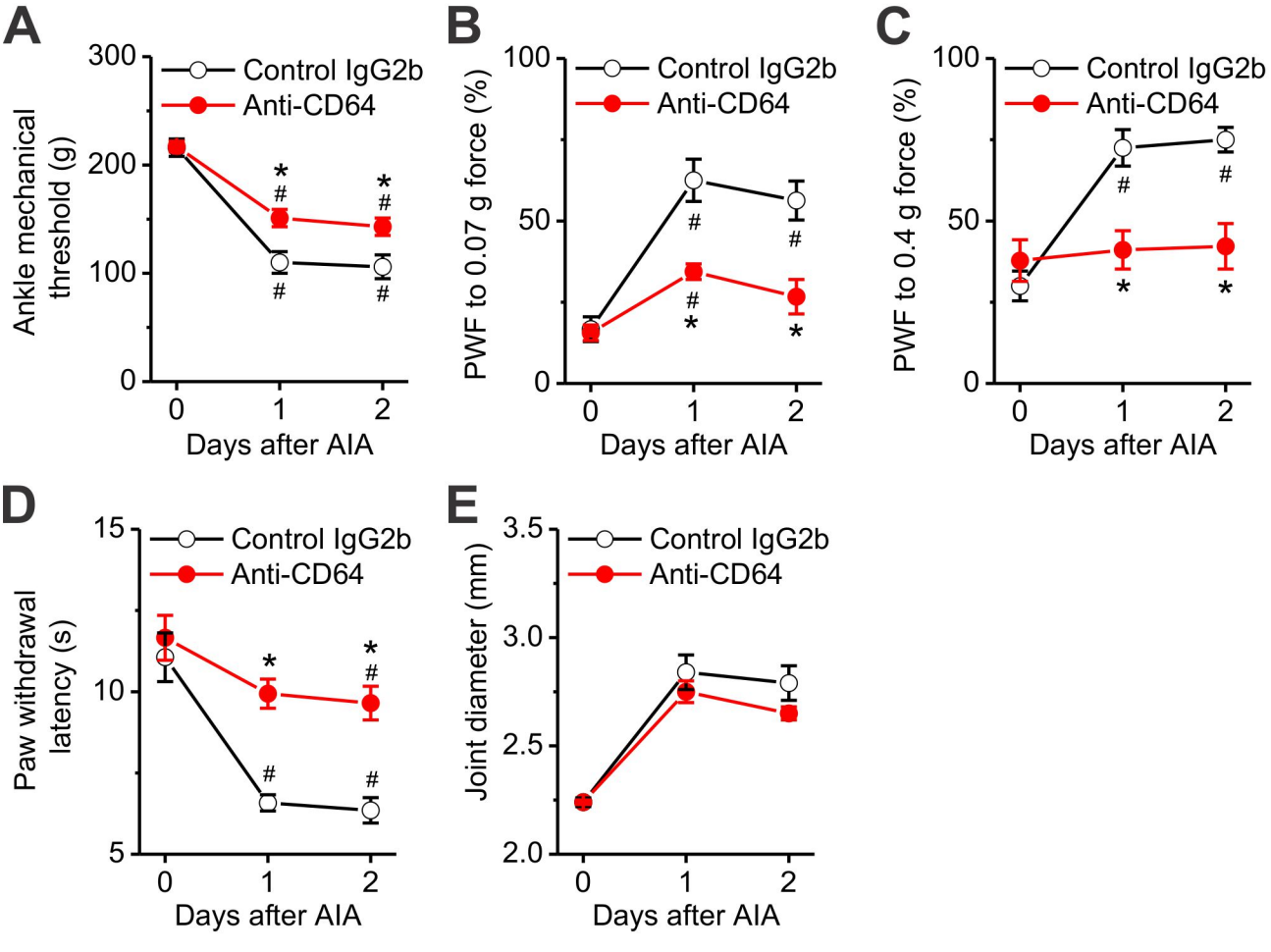
A
Ankle mechanical threshold (g)
300
200
100
0
Control IgG2b
Anti-CD64
0
1
2
Days after AIA
B
PWF to 0.07 g force (%)
100
50
0
Control IgG2b
Anti-CD64
0
1
2
Days after AIA
C
PWF to 0.4 g force (%)
100
50
0
Control IgG2b
Anti-CD64
0
1
2
Days after AIA
D
Paw withdrawal latency (s)
15
10
5
Control IgG2b
Anti-CD64
0
1
2
Days after AIA
E
Joint diameter (mm)
3.5
3.0
2.5
2.0
Control IgG2b
Anti-CD64
0
1
2
Days after AIA

Table S1. List of DNA primer sequences for quantitative real-time PCR

Target gene	Forward 5'-3'	Reverse 5'-3'
Il1b	GGAGAACCAAGCAACGACAAAATA	TGGGGAACTCTGCAGACTCAAAC
Il6	AAAGAG TTGTGCAATGGCAATTCT	AAGTGCATCATCGTTGTTCATACA
Tnfa	ATGAGAAGTTCCCAAATGGC	CTCCACTTGGTGGTTTGCTA
Mcp1	GAAGCTGTAGTTTTTGTCACCA	TTCCTTCTTGGGGTCAGCAC
Cxcl1	ATCCAGAGCTTGAAGGTGTTG	GTCTGTCTTCTTTCTCCGTTACTT
Mmp2	GACCAGGTTATCAGGGATGGCATTC	AAGTTCTGGAGATACAATGAAGTG
Mmp9	CTTCTGGCGTGTGAGTTTCC	ACTGCACGGTTGAAGCAAAGA
Mmp13	ACAAGCAGTTCCAAAGGCTACA	GCTGGGTCACACTTCTCTGG
Cd3	CGTCCGCCATCTTGGTAGAGAGAGCAT	CTACTGCTGTCAGGTCCACCTCCA
Cd68	ACCGCCATGTAGTCCAGGTA	ATCCCCACCTGTCTCTCTCA
Tpsb2	GAGCTTGAGGTCCCTGTGAA	GATAAGGAGGTGGGAGAGGC
Mcpt4	TCACCACTGAGAGAGGGTTCA	CATGAGCTCCAAGGGTGACA
Fcgr1	TGCTGGATTCTACTGGTGTGA	AAACCAGACAGGAGCTGATGA
Beta-actin	CTGAATGGCCCAGGTCTGA	CCCTGGCTGCCTCAACAC

Table S2. List of antibodies

Name	Dilution	Source	Identifier
Rat anti-CD3	1:50	BD Biosciences	Cat# 555273
Goat anti-cKit	1:200	R&D system	Cat# AF1356
Rat anti-CD68	1:500	BioLegend	Cat# 137001
Rat anti-Ly6C/G	1:50	BD Pharmingen	Cat# 550291
Rat anti-F4/80 (hybridoma supt)	1:25	ATCC	Cat# HB198
Rat anti-F4/80	1:200	Abcam	Cat# ab6640
Rabbit anti-NeuN	1:300	Abcam	Cat# ab177487
Chicken anti-NeuN	1:200	Aves	Cat# NUN
Rabbit anti-CGRP	1:500	Immunostar	Cat# 24112
Chicken anti-peripherin	1:200	Abcam	Cat# ab39374
Rabbit anti-NF200	1:1000	Sigma	Cat# N4142
Chicken anti-NF200	1:200	Aves	Cat# NFH
Rabbit anti-GS	1:1000	Abcam	Cat# ab49873
Sheep anti-DIG	1:200	Roche	Cat# 1133089001
Goat anti-rat IgG Alexa 488	1:500	Thermo Fisher Scientific	Cat# A11006
Donkey anti-rabbit IgG Cy3	1:500	Jackson ImmunoResearch labs	Cat# 711165152
Donkey anti-rabbit IgG Alexa 647	1:500	Jackson ImmunoResearch labs	Cat# 711605152
Donkey anti-goat IgG Alexa 494	1:500	Thermo Fisher Scientific	Cat# A11058
Donkey anti-sheep IgG Alexa 488	1:500	Abcam	Cat# Ab15077
Donkey anti-chicken IgG Cy3	1:500	Jackson ImmunoResearch labs	Cat# 703165155